Intramolecular Energy Transfer in Molecular Dyads Comprising Free-base Porphyrin and Ruthenium(II) Bis(2,2′:6′,2″-terpyridine) Termini

Andrew C. Benniston, Glen M. Chapman, Anthony Harriman,* and Maryam Mehrabi

Molecular Photonics Laboratory, School of Natural Sciences−Chemistry, Bedson Building, University of Newcastle, Newcastle upon Tyne, NE1 7RU, United Kingdom

Received: June 16, 2004; In Final Form: August 12, 2004

A molecular dyad has been synthesized in which free-base porphyrin and ruthenium(II) bis(2,2′:6′,2″-terpyridine) subunits are linked via a *meso*-phenylene group. The distal terpyridine ligand bears a single phenylethynylene group. Selective illumination into the metal complex is followed by rapid intramolecular triplet−triplet energy transfer from the metal-to-ligand charge-transfer (MLCT) triplet to the lowest-energy π,π^* triplet state localized on the porphyrin. This process is characterized by a reorganization energy of 0.14 eV and an electronic coupling matrix element of 76 cm^{-1}. Because of the alkynylene substituent, the initially produced MLCT state is centered on the distal terpyridine. Therefore, triplet energy transfer must cross the proximal terpyridine ligand. At low temperature, nuclear tunneling renders the rate of triplet energy transfer activationless. Upon selective illumination into the lowest-energy singlet (S_1) state localized on the porphyrin, fast singlet−triplet energy transfer occurs, to populate the MLCT triplet with high efficiency. This process happens by way of Dexter-type electron exchange at room temperature, and the MLCT triplet can be identified as a reaction intermediate at low temperature. The activation energy for singlet−triplet energy transfer is only 0.05 eV, because of the smaller energy gap, and the electronic coupling matrix element is decreased to 11 cm^{-1}, because energy transfer is spin-forbidden. At low temperature, dipole−dipole energy transfer becomes the main mechanism for decay of the porphyrin S_1 state. Excitation into the Soret band of the porphyrin is followed by rapid internal conversion to S_1 without energy or electron transfer to the appended metal complex.

Introduction

Considerable attention has been given to understanding the photophysical properties of molecular dyads formed from porphyrin and metal poly(pyridine) terminals.[1] These terminals have been linked by covalent frameworks,[2] through coordinative bonding[3] or via supramolecular networks,[4] and a variety of metal cations have been bound to either porphyrin or poly(pyridine) subunits. Light-induced energy-transfer and electron-transfer processes[5] have been observed in such dyads, at both ambient and low temperature, and certain dyads[6] react by way of the second-excited singlet state localized on the porphyrin subunit. Because the energy levels of the two terminals are similar, with singlet and triplet excited states being readily accessible, a multitude of photoprocesses become possible. Besides intramolecular electron transfer, triplet−triplet, triplet−singlet, and singlet−triplet energy transfer involving through-bond or through-space interactions have been described for various dyads and/or triads. Metal poly(pyridine) complexes have been shown to operate as relays for longer-range electron transfer between terminal porphyrins[7] and to mediate Dexter-type electron exchange[8] between different metalloporphyrins. It has been reported[6] that the mechanism of energy transfer is dependent on excitation wavelength, whereas related studies have shown that closely coupled dyads operate as second-harmonic generators.[9] Of particular interest has been the observation that light-induced electron transfer occurs with high efficiency in certain dyads at 77 K.[7]

* Author to whom correspondence should be addressed. E-mail address: anthony.harriman@ncl.ac.uk.

The richness of the photophysical properties of these porphyrin−poly(pyridine) dyads stems, in the main, from the facile modification of their energetics that can be attained by cation insertion into either subunit. Thus, energy transfer is favored by the free-base porphyrin; however, the corresponding zinc porphyrin readily undergoes oxidative electron transfer. Similar variations in redox properties can be obtained using different metal poly(pyridine) fragments. Within this class of dyads, metal bis(2,2′:6′,2″-terpyridine) complexes have found important applications as modules for the construction of linear arrays[10] and, in particular, they have been used as the bridge for porphyrin-based triads. Unfortunately, the triplet lifetime of ruthenium(II) bis(2,2′:6′,2″-terpyridine) is too short for this complex to be a useful sensitizer or energy relay,[11] except where the subunits are maintained in close proximity. The triplet lifetime is greatly enhanced by substitution of an alkynylene group at the 4′-position of the terpyridyl ligand,[12] and such metal complexes have been linked directly to the porphyrin ring via the meso-position.[9] Here, we have adopted a somewhat different strategy and attached an alkyne substituent to the distal terpyridine ligand. The net result is that the triplet lifetime of the ruthenium(II) bis(2,2′:6′,2″-terpyridine) subunit is prolonged to such an extent that this species operates as an energy relay. We now describe the results of a temperature-dependence examination of the various energy-transfer steps that occur in the dyad formed between this alkynylene-substituted ruthenium(II) bis(2,2′:6′,2″-terpyridine) subunit and a free-base porphyrin. The latter unit was selected to preclude intramolecular electron transfer.

10.1021/jp047400j CCC: $27.50
Published on Web 09/25/2004

SCHEME 1: General Methodology Used to Prepare the Molecular Dyad Studied in This Work

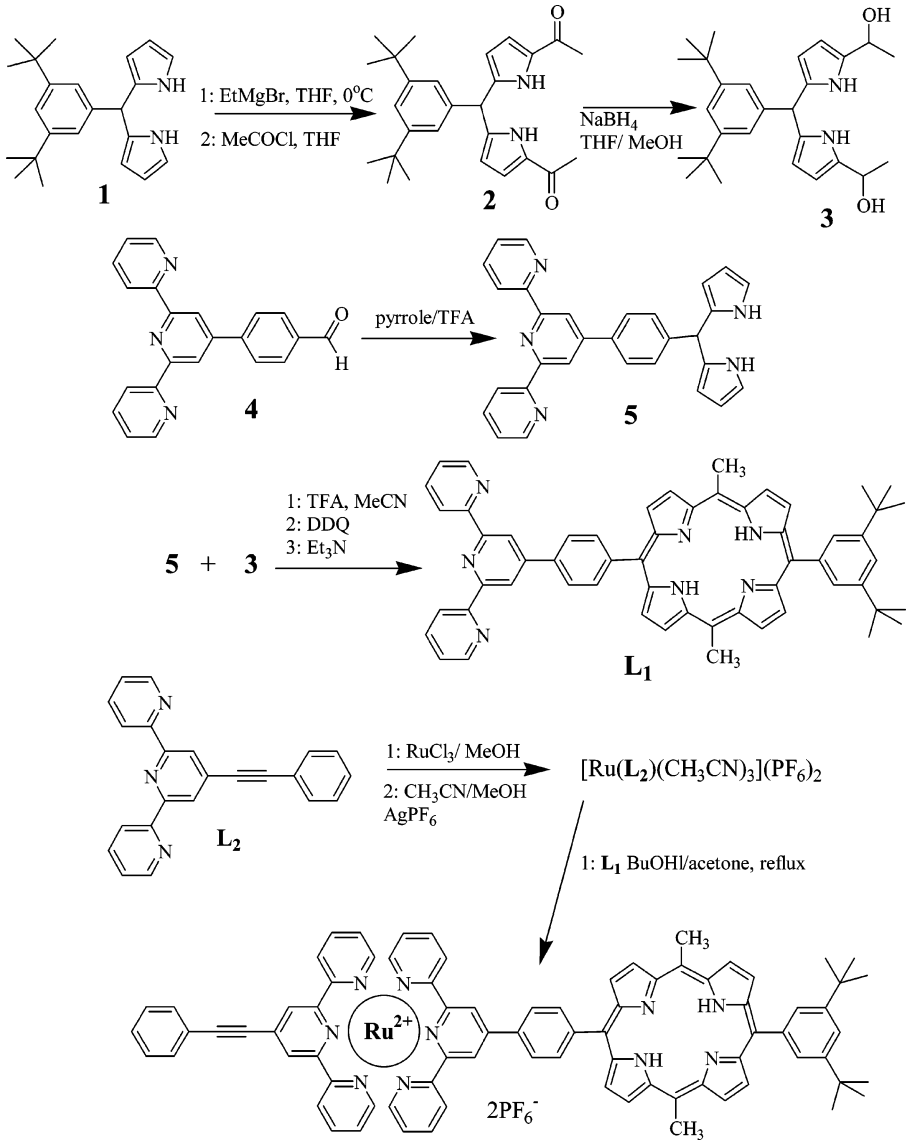

Experimental Section

All raw materials were purchased from Aldrich Chemical Co. and were used as received. Solvents were dried by standard literature methods before being distilled and stored under nitrogen over 4 Å molecular sieves. ^{1}H and ^{13}C NMR spectra were recorded with a JEOL model Lambda 500 spectrometer. Routine mass spectra and elemental analyses were obtained using in-house facilities. The starting materials **1**,[13] **4**,[14] **L$_2$**,[15] and **[Ru(L$_2$)(CH$_3$CN)$_3$](PF$_6$)$_2$**[16] were prepared and purified by literature methods. All melting points are uncorrected. The overall procedure used for the synthesis of dyad **D1** is given in Scheme 1.

Preparation of 1-{5-[(5-acetyl-1H-pyrrol-2-yl)-3,5-(di-*tert*-butylphenyl)-methyl]-1H-pyrrol-2-yl}-ethanone (2). A solution of **1** (4.00 g, 12.0 mmol) in dry toluene (240 mL) was cooled to 0 °C under a N_2 atmosphere. Ethylmagnesium bromide in tetrahydrofuran (THF) (1 M, 60 mL, 60.0 mmol), was added to this solution dropwise, while maintaining the solution at a temperature of 0−5 °C. The solution was warmed to room temperature and stirred for a further 30 min. The mixture was again cooled to 0 °C and a solution of acetyl chloride (2.36 g, 30.0 mmol) in dry toluene (30 mL) was added dropwise while maintaining the temperature at 0−5 °C. After allowing the solution to warm to room temperature, it was stirred for an additional 30 min and quenched by addition of saturated ammonium chloride solution (180 mL). The organic layer was washed with brine (200 mL) and distilled water (2 × 200 mL) and then was separated. The organic residues were dried over $MgSO_4$ and then filtered and evaporated under reduced pressure. The crude product was dissolved in methanol (200 mL) and distilled water (100 mL) was added slowly to afford a precipitate that was isolated by filtration. A further portion of distilled water (100 mL) was added to the mother liquor to afford a second crop of solid precipitate, which was filtered and combined with the main fraction. The compound was recrystallized from an aqueous methanol solution to produce white crystals (yield 2.05 g, 45%). Melting point: mp = 88 °C. ^{1}H NMR ($(CD_3)_2SO$): δ 11.78 (s, 2H, N*H*), 7.25 (s, 1H, Ar*H*), 7.08 (s, 2H, Ar*H*), 6.89 (s, 2H, Pr), 6.89 (s, 2H, Pr), 5.94 (s, 2H, Pr), 5.54 (s, 1H, C*H*), 2.29 (s, 6H, CH_3), 1.23 (s, 18H, C(CH_3)$_3$). ^{13}C NMR ($(CD_3)_2SO$): δ 186.9, 150.3, 141.1, 140.7, 131.7, 122.7, 120.5, 117.6, 109.2, 43.7, 34.8, 31.6, 25.6. EI-MS (M^+) *m*/*z* Calcd for $C_{27}H_{34}N_2O_2$, 418.2620. Found: 418.2609. Elemental Anal. Calcd (%) for $C_{27}H_{34}N_2O_2$: C, 77.48; H, 8.19; N, 6.69. Found: C, 77.15; H, 8.31; N, 6.52.

Preparation of 1-{5-[(5-acetyl-1*H*-pyrrol-2-yl)-3,5-(di-*tert*-buylphenyl)-methyl]-1*H*-pyrrol-2-yl}-ethanol (3). A solution of **2** (1.85 g, 4.40 mmol) in tetrahydrofuran (THF) (280 mL) and methanol (90 mL) was stirred in an air environment for 5 min. $NaBH_4$ (8.36 g, 221 mmol) was added carefully to this vigorously stirred solution over a 5-min period. (Caution: A violent release of hydrogen gas occurs during this process.) The mixture was stirred for an additional 2 h, followed by the careful addition of distilled water (75 mL). After stirring the solution for 10 min, the product was extracted with dichloromethane (400 mL). The organic layer was washed with distilled water (2×200 mL), separated, dried over Na_2CO_3, and filtered. Removal of the organic solvents under reduced pressure afforded orange-yellow crystals (yield 1.68 g, 90%). Melting point: mp = 70 °C. ^{1}H NMR ($CDCl_3$) δ = (2H, s, N*H*), 7.20 (1H, s, Ar*H*), 7.09 (2H, s, Ar*H*), 5.71 (2H, s, Py*H*), 5.58 (2H, s, Py*H*), 5.24 (1H, s, C*H*), 4.81 (2H, J = 5 Hz, O*H*), 4.64 (2H, m, J = 6 Hz, C*H*), 1.34 (6H, t, J = 6 Hz, CH_3), 1.24 (18H, s, C(CH_3)$_3$). ^{13}C NMR ($CDCl_3$) δ = 149.8, 143.2, 136.2, 133.1, 122.7, 119.7, 105.5, 103.2, 62.7, 44.4, 34.8, 31.7, 23.9. EI-MS (M^+) m/z Calcd for $C_{27}H_{38}N_2O_2$: 422.2933. Found: 422.2925. Elemental Anal. Calcd (%) for $C_{27}H_{38}N_2O_2$: C, 76.74; N, 6.63; H, 9.06. Found: C, 76.57; N, 6.04; H, 9.28.

Preparation of 4′-{4-[bis-(1*H*-pyrrol-2-yl)-methyl]-phenyl}-[2,2′:6′,2″]-terpyridine (5). A mixture of 4-[2,2′:6′,2″]terpyridin-4′-yl-benzaldehyde (4.50 g, 13.3 mmol), trifluoroacetic acid (0.15 g, 1.31 mmol) and pyrrole (22.32 g, 0.33 mmol) was stirred at 70 °C under N_2 for 45 min. The mixture was then cooled to room temperature and the excess pyrrole removed at 40 °C under reduced pressure. The resultant product was chromatographed using basic alumina and ethyl acetate/dichloromethane (1:4) as the eluant. The resultant yellow product was recrystallized from toluene to produce off-white crystals (1.34 g, 22%). Melting point: mp = 200 °C. ^{1}H NMR ($(CD_3)_2SO$): δ 10.66 (s, 2H, N*H*), 8.76 (dd, 2H, J = 5, J′ = 1 Hz, Py*H*), 8.70 (s, 2H, Py*H*), 8.67 (d, 2H, Py*H*), 8.02 (t, 2H, J = 8 Hz, Py*H*), 7.86 (d, 2H, J = 8 Hz, Ar*H*), 7.53 (dd, 1H, J = 5 Hz, J′ = 1 Hz, Py*H*), 7.50 (dd, 1H, J = Hz, J′ = 1 Hz, Py*H*), 7.41 (d, 2H, J = 8 Hz, Ar*H*), 6.66 (s, 2H, Pr*H*), 5.95 (s, 2H, Pr), 5.70 (s, 2H, Pr*H*), 5.48 (s, 1H, C*H*). ^{13}C NMR ($(CD_3)_2SO$): δ 156.0, 155.3, 149.7, 145.7, 137.8, 135.7, 133.1, 129.5, 127.0, 124.9, 121.3, 118.1, 117.4, 107.3, 106.6, 49.0, 43.6. EI-MS (M^+) m/z Calcd for $C_{30}H_{23}N_5$: 453.1953. Found: 453.1965. Elemental Anal. Calcd (%) for $C_{30}H_{23}N_5 \cdot 0.5C_7H_8$: C, 80.54; H, 5.45); N, 14.02. Found: C, 80.32; H, 5.37; N, 14.78.

Preparation of 5-(3,5-di-*tert*-butylphenyl)-10,20-dimethyl-15-(4-[2,2′:6′,2″]-terpyridin-4-yl-phenyl)-porphyrin (L_1). Compounds **5** (0.23 g, 0.55 mmol) and **3** (0.25 g, 0.55 mmol) in N_2-purged acetonitrile (220 mL) were stirred for 5 min under N_2. To this stirred solution was added trifluoroacetic acid (0.76 g, 6.71 mmol) over a period of 5−10 s. The mixture was protected from light and stirred for an additional 45 min. The oxidant 2,3-dichloro-5,6-dicyanoquinone (0.38 g, 1.62 mmol) was added and the solution stirred for 2 h. Triethylamine (0.67 g, 6.71 mmol) was added and the solution stirred for an additional 5 min. Removal of the solvent under reduced pressure afforded a crude product that was purified by column chromatography (basic alumina) using dichloromethane as eluant. After removal of a pale pink fraction, the eluant was changed to dichloromethane:ethyl acetate (95:5) which afforded, after solvent removal, a dark purple product (yield 55 mg, 12%). Mp > 250 °C. ^{1}H NMR ($CDCl_3$): δ 9.38 (dd, 4H, J = 7 Hz, J′ = 5 Hz), 9.00 (s, 2H), 8.83 (dd, 4H, J = 5 Hz, J′ = 3 Hz), 8.73 (d, 2H, J = 4 Hz), 8.67 (d, 2H, J = 8 Hz), 8.24 (dd, 4H, J = 15 Hz, J ‘ = 8 Hz), 7.99 (d, 2H, J = 2 Hz), 7.84 (t, 2H, J = 8 Hz), 7.75 (t, 1H, J = 2 Hz), 7.3 (t, 2H, J = 6 Hz), 4.53 (6H, s, CH_3), 1.47 (18H, s, C(CH_3)$_3$), −2.61 (s, 2H, N*H*). EI-MS (M^+) m/z Calcd for $C_{57}H_{50}N_7$: 833.4206. Found: 833.4203. Elemental Anal. Calcd. (%) for $C_{57}H_{50}N_7 \cdot 2H_2O$: C, 78.68; H, 6.37; N, 11.27. Found: C, (78.15; H, 6.03; N, 11.02.

Preparation of the Dyad D1. A solution of **[Ru(L_2)(CH_3-CN)$_3$](PF_6)$_2$** (42 mg, 0.059 mmol) and **L_1** (49 mg, 0.059 mmol) in butanol (50 mL) and acetone (20 mL) was refluxed gently under a N_2 atmosphere for 24 h. The solvent was evaporated under reduced pressure and the crude product was purified by column chromatography (basic alumina) with diethyl ether: acetonitrile mixture (3:1) as the eluant. After removal of a (faint) purple fraction, the eluant was changed to diethyl ether: acetonitrile (1:1) to elute a pink fraction. The eluant was then changed to acetonitrile. Evaporation of the red fractions produced a solid that was further purified by slow vapor diffusion of diethyl ether into an acetonitrile solution of the crude material (yield: 20 mg, 22%). Mp > 250 °C. ^{1}H NMR (CD_3CN): δ 9.55 (4H, dd, J = 5 Hz, J′ = 19 Hz), 9.30 (1H, s), 8.91 (2H, d, J = 5 Hz), 8.87 (1H, s), 8.80 (2H, d, J = 5 Hz), 8.76 (2H, d, J = 8 Hz), 8.59 (2H, d, J = 8 Hz), 8.50 (3H, d, J = 8 Hz), 8.44 (1H, d, J = 8 Hz), 8.04 (1H, d, J = 2 Hz), 7.96−7.88 (4H, m), 7.79−7.71 (3H, m), 7.54−7.52 (4H, m), 7.41 (2H, d, J = 5 Hz), 7.34 (1H, d, J = 5 Hz), 7.24−7.10 (5H, m), 4.73 (6H, s, CH_3), 1.43 (18H, s, C(CH_3), −2.45 (2H, s, N*H*). UV−visible: λ_{MAX}/nm (ϵ/M^{-1} cm^{-1}): 655 (2100), 500 (18 500), 422 (46 200), 318 (34 760); ES-MS (M-PF_6^+) m/z Calcd for $C_{80}H_{66}N_{10}RuPF_6$: 1413.4. Found, 1413.6. (M-2PF_6^+) m/z Calcd for $C_{80}H_{66}Ru$: 634.2. Found: 634.1. Elemental Anal. Calcd (%) for $C_{80}H_{66}N_{10}RuP_2F_{12} \cdot HPF_6$: C, 56.37; H, 3.96; N, 8.22. Found: C, 56.10; H, 3.66; N, 8.37.

Absorption spectra were recorded with a Hitachi model U3310 spectrophotometer, and luminescence spectra were recorded with a fully corrected Yvon-Jobin model Fluorolog τ-3 spectrophotometer. Emission spectra were recorded for optically dilute solutions after purging with N_2. Luminescence quantum yields were determined relative to *meso*-tetraphenylporphyrin[17] (Φ_F = 0.12) in toluene or osmium(II) bis(2,2′:6′,2″-terpyridine)[18] (Φ_{LUM} = 0.014) in acetonitrile. Temperature dependence studies were made with sealed sample cells housed in an Oxford Instruments model Optistat DN cryostat. Emission lifetimes were measured at room temperature with the τ-3 spectrophotometer. For lower temperatures, the luminescence lifetimes were measured via time-correlated, single-photon counting, using a synchronously pumped, cavity-dumped, mode-locked dye laser (full width at half maximum (fwhm) of 6 ps) as an excitation source. The dye laser was tuned to an appropriate excitation wavelength. Emission was isolated from scattered laser light with a high-radiance monochromator and detected with a microchannel plate photocell. After deconvolution of the instrument response function, the time resolution of this setup was ca. 40 ps. The spectral resolution, being limited by the need to obtain a reasonable count rate, was ca. 4 nm.

Flash photolysis studies were made with a mode-locked, frequency-doubled Nd:YAG laser (fwhm = 20 ps). The excitation pulse was passed through a Raman shifter, to isolate the required wavelength. The monitoring pulse was a white light continuum, delayed with respect to the excitation pulse with a computer-controlled, optical delay line. The two pulses were directly almost collinearly through the sample cell. The monitoring pulse was dispersed with a Princeton Instruments spectrograph and detected with a dual-diode array spectrometer. Approximately 150 individual laser shots were averaged at each

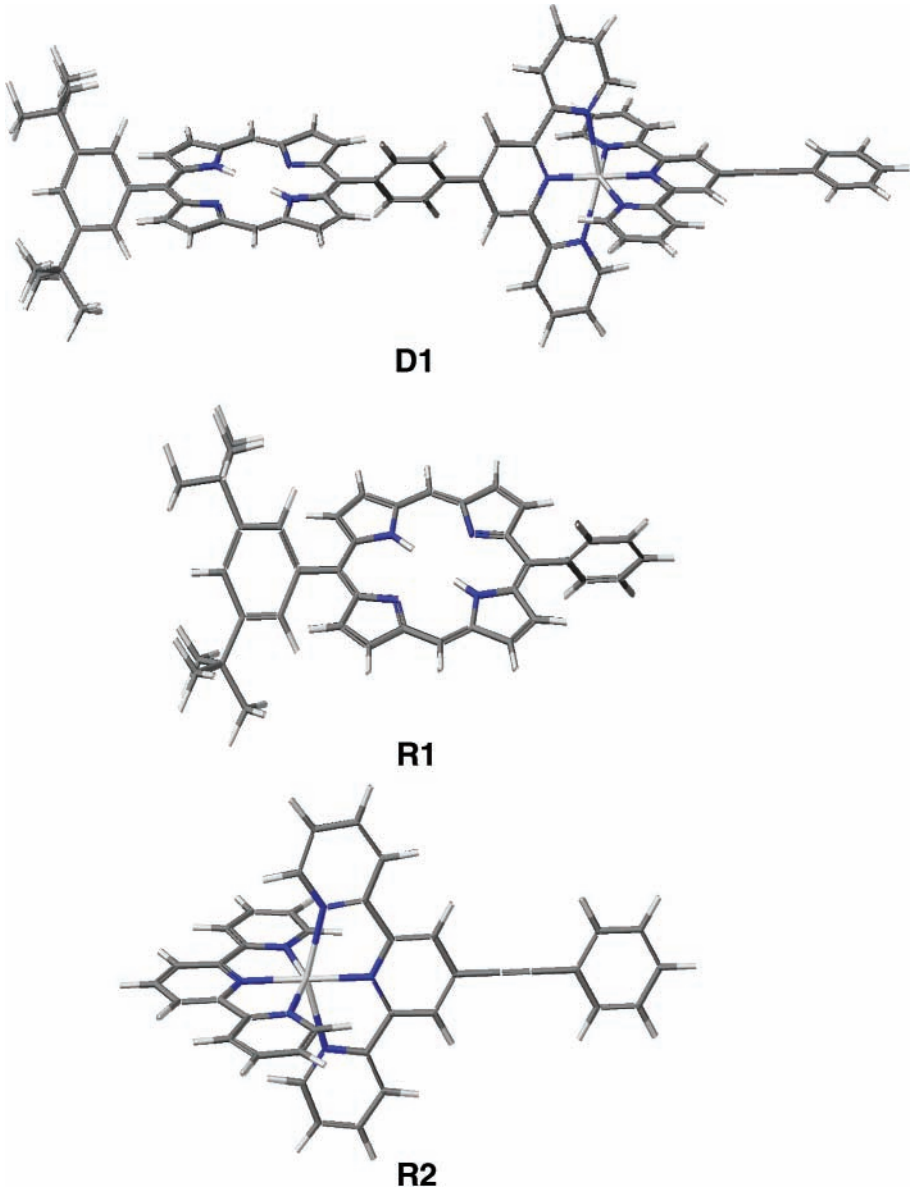

Figure 1. Energy-minimized structures of the dyad **D1**, the free-base porphyrin reference compound **R1**, and the Ru-terpy reference compound **R2**.

delay line. Kinetic measurements were made by overlaying spectra collected at different delay times. For long-lived transients, a pulsed xenon arc lamp was used as the monitoring beam and a fast response photomultiplier tube (PMT) was used as the detector. Approximately 10 individual records were averaged at each wavelength. All measurements were made with dilute solutions after purging with N_2.

Electrochemical measurements were made with an HCH electrochemical analyzer. The working electrode was a highly polished glassy carbon disk, and the counter electrode was a platinum wire. An Ag/AgCl reference electrode was used. The solution (ca. 1 mM) contained tetra-*N*-butylammonium hexafluorophosphate (0.2 M) as the background electrolyte and was purged thoroughly with N_2 prior to electrolysis. Reduction potentials were reproducible to within 15 mV.

Results and Discussion

Synthesis. Preparation of multitopic porphyrin-2,2′:6′,2″-terpyridine molecular dyads has been developed by Sauvage and co-workers,[2d,2f,8] using a one-pot condensation approach. This method reduces the number of precursors required but relies on careful chromatography to separate the variety of products so obtained. In contrast to this method, outlined in Scheme 1 is the synthetic procedure used for the preparation of $\mathbf{L_1}$ and the corresponding ruthenium(II) bis(2,2′:6′,2″-terpyridine) complex (**D1**). The methodology used is an adaptation of that reported by Lindsey and co-workers[19] for the synthesis of multifunctional porphyrins. This method was specifically chosen because it is highly adaptable and allows the preselection of groups to be appended at the meso sites, because two dipyrromethene units are coupled together in the final step. Thus, the known compound **1**[13] was converted to the diketone **2** by selective deprotonation of the two pyrrole units and subsequent reaction with acetyl chloride. Reduction of the carbonyl groups to secondary alcohols proceeded smoothly, to afford compound **3** in reasonable yield. The second half of the porphyrin unit 5 was constructed by condensation of the benzaldehyde-substituted 2,2′:6′,2″-terpyridine **4** with excess pyrrole. Condensation of **5** with **3**, followed by oxidation with 2,3-dichloro-5,6-dicyanoquinone, afforded ligand $\mathbf{L_1}$ in 12% overall yield after purification by column chromatography on basic alumina. The ruthenium(II) cation was introduced into $\mathbf{L_1}$ to afford the required

TABLE 1: Reduction Potentials and Energy Levels Measured for Dyad D1 and for the Two Reference Compounds in *N,N*-Dimethylformamide (DMF) Solution at Room Temperature

	value		
property	**D1**	**R1**	**R2**
E_{OX}/V vs Ag/AgCl	0.90 (1e); 1.35 (1e)	0.92 (1e)	1.33 (1e)
E_{RED}/V vs Ag/AgCl	−1.09 (1e), −1.34 (1e), −1.40 (1e), −1.60 (1e)	−1.32 (1e), −1.55 (1e)	−1.11 (1e), −1.43 (1e)
E_S (eV)	1.88	1.89	2.53
E_T (eV)	1.93,[a] 1.47[b]	1.47	1.93
E_S^{OX}/V vs Ag/AgCl	−0.98[c]	−0.97	
E_S^{RED}/V vs Ag/AgCl	0.54[d]	0.57	
E_T^{OX}/V vs Ag/AgCl	−0.84[e]		−0.82
E_T^{RED}/V vs Ag/AgCl	0.58[f]		0.60
ΔG^0_S(RED) (eV)[g]	+0.69		
ΔG^0_S(OX) (eV)[h]	+0.15		
ΔG^0_T(RED) (eV)[i]	+0.20		
ΔG^0_T(OX) (eV)[j]	+0.54		

[a] Refers to the MLCT triplet state. [b] Refers to the π,π^* triplet state associated with the porphyrin. [c] Oxidation potential calculated for the first-excited singlet (S_1) state of the porphyrin. [d] Reduction potential calculated for the first-excited singlet (S_1) state of the porphyrin. [e] Oxidation potential calculated for the MLCT triplet (T_1) localized on the metal complex. [f] Reduction potential calculated for the MLCT triplet (T_1) localized on the metal complex. [g] Refers to reduction of S_1. [h] Refers to oxidation of S_1. [i] Refers to reduction of the MLCT triplet. [j] Refers to oxidation of the MLCT triplet.

dyad **D1** by attachment of $[Ru(L_2)(CH_3CN)_3](PF_6)_2$ to the free 2,2′:6′,2″-terpyridine site. All compounds were fully characterized by standard analytical techniques, including ^1H and ^{13}C NMR, electrospray mass spectrometry (ES-MS), and elemental analysis. Structural formulae of the main compounds are provided in Figure 1.

Several features should be noted about the structure of the **D1** dyad. The compound is similar to dyads studied earlier by other researchers[5] and is characterized by the close positioning of the subunits. The center-to-center distance is only 9.3 Å, whereas the edge-to-edge separation between porphyrin and distal pyridine rings is 7.8 Å.[20] A key feature of **D1** concerns the presence of the phenylethynylene substituent attached at the distal 4′-position. Previous work has shown that this substituent favors electron delocalization at the triplet level[21] and reduces the triplet energy, because of its electron-withdrawing character.[22] The lowest-energy triplet state associated with the metal complex is formed by charge injection into the alkynylene-substituted terpyridine ligand from the metal center. In the **D1** dyad, this has the effect of directing charge away from the appended porphyrin. Thus, excited-state interactions involving the latter triplet will be somewhat unfavorable. A further disparity between **D1** and earlier dyads[2,5] is that the pyrrole rings remain unsubstituted. This strategy provides for increased rotational freedom for the *meso*-phenylene rings[1] and minimizes structural distortion of the porphyrin nucleus. The average torsion angle between porphyrin and phenylene rings is 44°, as measured by molecular modeling studies.[20]

Energy Levels and Reduction Potentials. For **R2**, which is the reference compound for the ruthenium moiety,[23] the metal center undergoes a quasi-reversible oxidation wave, with a half-wave potential of +1.33 V vs Ag/AgCl. There are two reversible reduction processes, corresponding to half-wave potentials of −1.11 and −1.43 V vs Ag/AgCl, respectively. The first reduction step can be attributed to the addition of one electron to the substituted terpyridine ligand, whereas the second step is due to the one-electron reduction of the parent terpyridine ligand. The free-base porphyrin reference (**R1**) shows a reversible one-electron oxidation step with a half-wave potential of +0.92 V vs Ag/AgCl whereas the half-wave potential for one-electron reduction of the porphyrin ring is −1.32 V vs Ag/AgCl. Similar processes were observed for dyad **D1** and the derived reduction potentials are collected in Table 1. These values remain comparable to those observed for the reference compounds, thereby facilitating assignment and suggesting there the two subunits are not in strong electronic communication, despite their close proximity.

The absorption spectrum recorded for dyad **D1** in *N,N*-dimethylformamide (DMF) is given in Figure 2 and shows three important regions of interest: (i) the Q-band, which lies between 540 and 660 nm, corresponds to population of the first-excited singlet state of the porphyrin; (ii) the metal-to-ligand charge-transfer (MLCT) transition localized on the metal complex is centered at 500 nm, although there is some overlap with absorption bands associated with the porphyrin subunit; and (iii) the Soret band of the porphyrin is seen as an intense transition centered around 420 nm and characterizes promotion to the second-excited singlet state of the porphyrin. There are other bands at <400 nm, which can be attributed to $\pi-\pi^*$ transitions localized on the terpyridyl ligands.[23] The main absorption bands found for the dyad display a slight broadening and red shift, compared to the relevant transitions identified for the reference compounds (see Figure 2). In particular, the Soret band is considerably less intense than that of **R1**. This spectral perturbation results from the close coupling of the chromophores.

The excited singlet (E_S) and triplet (E_T) state energies for **R1** and **R2** were calculated from emission spectra. For **R1**, the intersection of normalized absorption and emission spectra was used to estimate E_S, whereas E_T for **R2** has been reported previously[15,23] (see Table 1). Very weak phosphorescence could be detected for **R1** in an ethanol glass at 77 K in the presence of 15% iodoethane. The (0,0) transition was taken as being representative of E_T for the free-base porphyrin. The derived value (see Table 1) is comparable to that reported earlier for a free-base porphyrin;[24] however, the large slit widths needed for this experiment do not favor accurate determination of the triplet energy. Reduction potentials for the various excited states were calculated from the ground-state reduction potentials and the relevant excitation energies.[25] These values are collected in Table 1.

Based upon the derived data, some conclusions can be determined, with respect to putative intramolecular excited-state processes. Thus, it is most unlikely that light-induced electron transfer will compete with inherent deactivation of either the first singlet (S_1) or first triplet (T_1) excited states of the free-base porphyrin subunit. Similarly, the MLCT triplet state localized on the metal complex lacks the redox power to oxidize or reduce the appended porphyrin ring. Moreover, the porphyrin

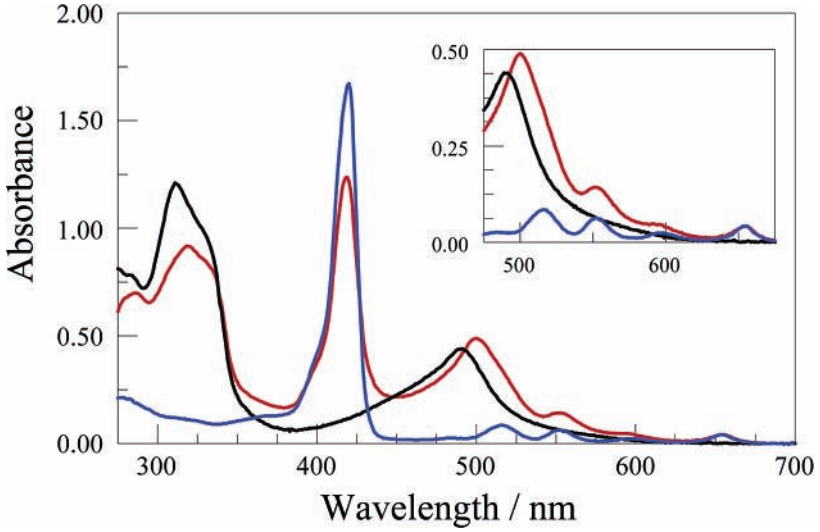

Figure 2. Absorption spectra recorded for the dyad **D1** (red curve), the porphyrin reference **R1** (blue curve), and the Ru-terpy reference **R2** (black curve) in *N*,*N*-dimethylformamide (DMF). The insert shows an expansion of the Q-band region of the spectra.

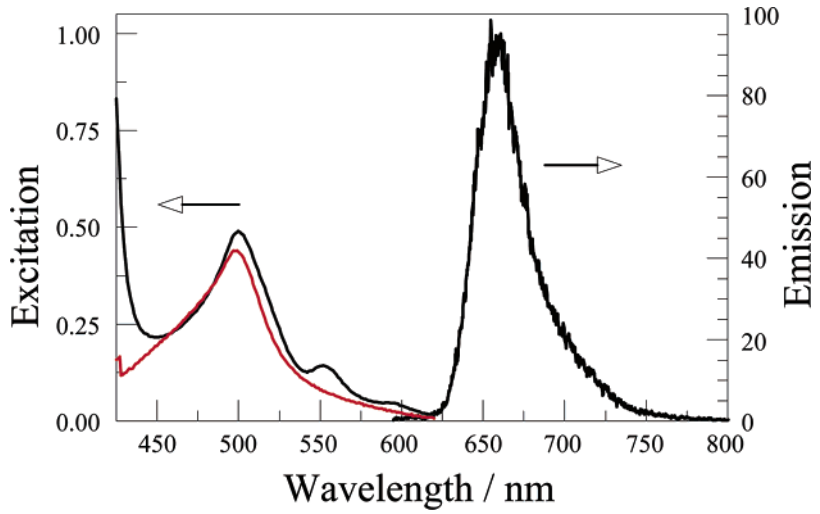

Figure 3. Luminescence spectrum recorded for dyad **D1** following excitation at 490 nm and a comparison of the absorption and excitation (shown in red) spectra.

T_1 state represents the lowest-energy metastable species in this system and could be populated by intramolecular triplet energy transfer from the MLCT triplet state. The porphyrin S_1 state lies at a slightly higher energy than that of the MLCT triplet, such that these two species might be involved in singlet-to-triplet or triplet-to-singlet energy-transfer processes, respectively.

Preferential Excitation into the Ruthenium(II) Bis(2,2′:6′,2″-terpyridine) Subunit. The MLCT transition localized on the metal complex exhibits a pronounced absorption maximum at ~490 nm (see Figure 2) where the free-base porphyrin subunit shows little, if any, absorption. Excitation of the reference compound **R2** at this wavelength results in luminescence centered at 650 nm.[15,23] The emission quantum yield and lifetime measured for **R2** in deoxygenated butyronitrile at room temperature are 0.00036 and 44 ns, respectively. The **D1** dyad displays a similar luminescence spectrum when excited at 490 nm (Figure 3), but the quantum yield is very low and the emission lifetime is reduced to ca. 500 ps. The quantum yield is too low to be measured accurately, because the integrated luminescence spectral profile is only ca. 2% of that measured for an optically matched solution of **R2**. The corrected excitation spectrum recorded for dyad **D1** under these conditions (Figure 3) is remarkably similar to that found for **R2** and shows, in particular, that photons absorbed by the free-base porphyrin subunit to not contribute to luminescence from the MLCT triplet state of the appended metal complex. It is also clear from the measured emission lifetimes that the triplet MLCT state in the dyad is heavily quenched, with respect to that in the reference compound. Even so, luminescence from the MLCT triplet decayed via first-order kinetics at all monitoring wavelengths. Comparing the triplet lifetimes measured for the two compounds in deoxygenated solutions indicates that the rate constant for intramolecular quenching is ca. 2×10^9 s^{-1} at room temperature.

Having established that intramolecular electron transfer to or from the MLCT triplet state localized on the metal complex is unlikely for dyad **D1**, it seems reasonable to suppose that quenching results from electronic energy transfer to the appended porphyrin. In principle, energy transfer could occur to both S_1 and T_1 excited π,π^* states localized on the porphyrin subunit. Both processes are thermodynamically favorable; triplet−singlet energy transfer from the MLCT state to S_1 is weakly exoergonic ($\Delta G° = -0.05$ eV), whereas triplet−triplet energy transfer from the MLCT state to T_1 is strongly exoergonic ($\Delta G° = -0.46$ eV). However, comparison of the corrected excitation and absorption spectra recorded for **D1**, measured for emission from the porphyrin S_1 singlet state (Figure 4), shows that photons absorbed directly by the metal complex are not transferred to the porphyrin S_1 state. This

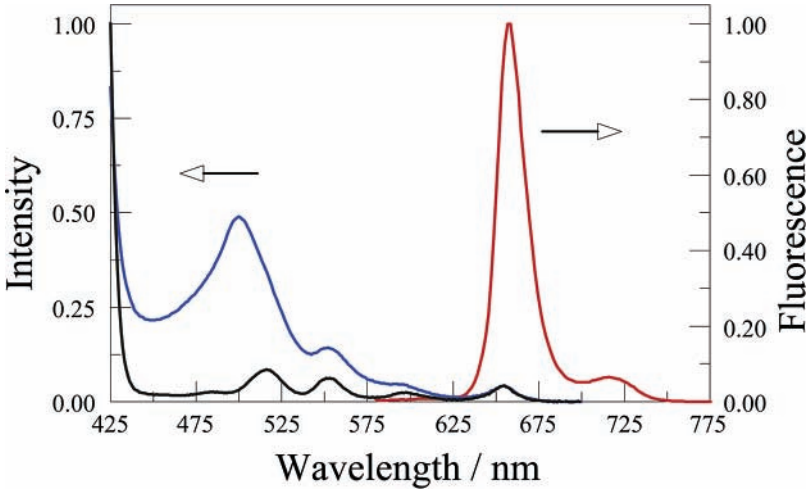

Figure 4. Fluorescence spectrum recorded for dyad **D1** following excitation at 590 nm (red curve). Also shown is a comparison of the absorption spectrum (blue curve) and the excitation spectrum (black curve) recorded for the dyad.

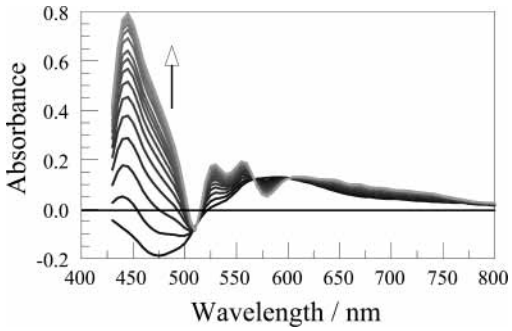

Figure 5. Transient absorption spectra recorded after laser excitation of dyad **D1** at 470 nm. Note that the signal at ~470 nm is initially negative but becomes positive with increasing delay time.

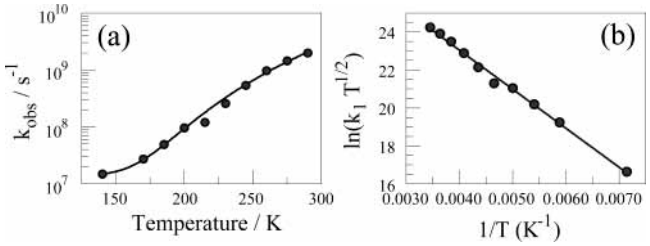

Figure 6. (a) Effect of temperature on the observed rate constant for triplet−triplet energy transfer in dyad **D1**. (b) The derived activated rate constant (k_1), replotted according to eq 2.

finding suggests that energy transfer to S_1 is not important in this system and accounts for <5% of the total deactivation processes available to the MLCT triplet state.

Laser flash photolysis of **D1** in deoxygenated DMF solution with excitation at 470 nm results in a transient differential absorption spectrum (Figure 5) that closely resembles that characterized earlier for the MLCT triplet excited state of **R2**.[15] The spectrum shows pronounced bleaching of the MLCT transition centered at 490 nm. This triplet state decays over some hundreds of picoseconds to form the π,π^* triplet state localized on the porphyrin subunit. The rate constant for this process ($k_{TT} = 2 \times 10^9$ s^{-1}) is in exact agreement with the rate constant for decay of the MLCT triplet state measured by time-resolved emission spectroscopy. The spectral records provide clear evidence for intramolecular triplet−triplet energy transfer. Decay of the porphyrin T_1 state occurs via first-order kinetics with a rate constant of 5×10^3 s^{-1} in deoxygenated solution at room temperature.

Triplet−triplet energy transfer has been reported for related dyads.[5] Thus, for a system having the reactants linked directly at the meso-position,[5b,5c] the rate constant for triplet energy transfer from the MLCT state to the porphyrin π,π^* triplet was $>5 \times 10^{10}$ s^{-1} at room temperature. For the dyad having the two reactants separated by a phenylene ring,[5a] k_{TT} was observed to be 2.2×10^8 s^{-1} at 77 K; however, this process could not be resolved from the rapid ($k = 1.2 \times 10^{10}$ s^{-1}) internal conversion from the triplet MLCT to the ground state, observed at room temperature. Note that, in the case of dyad **D1**, the initial MLCT triplet is formed by charge injection into the distal terpyridyl ligand. This means that triplet energy transfer occurs over a somewhat increased separation distance, compared to the other dyads mentioned here.[5] None of these dyads[5] provided clear evidence for triplet−singlet energy transfer from the MLCT state to the porphyrin S_1 level. This process, which probably occurs via the Förster mechanism, is not favored by either the very small overlap integral or the poor photophysical properties associated with the donor triplet.

Following excitation of the **D1** dyad in butyronitrile at 490 nm, the luminescence spectrum characteristic of the metal complex was monitored, as a function of temperature. It was found that the emission yield increased as the temperature decreased, as reported earlier for the reference complex[15,23] (see Supporting Information). The emission yield showed a nonlinear dependence on temperature (see Supporting Information) but, even at low temperature, the value was much less than that recorded for **R2** under identical conditions. The variation in triplet lifetime mirrored the change in quantum yield, and it is worth noting that the decay profile remained strictly mono-exponential at all temperatures and at all monitoring wavelengths. This variation in triplet lifetime can be used to calculate the rate constant (k_{TT}) for triplet−triplet energy transfer as a function of temperature. The derived rate constants are activated in the high-temperature limit but become activationless as the medium becomes frozen (Figure 6a). Within the glass, k_{TT} has a constant value of 1.4×10^7 s^{-1}. The entire data set can be fit to a generic equation of the type

$$k_{TT} = k_0 + k_1 \exp\left(-\frac{E_A}{RT}\right) \qquad (1)$$

where k_0 is the activationless rate constant ($k_0 = 1.4 \times 10^7$ s^{-1}), E_A is the activation energy, and k_1 refers to the activated rate constant for triplet energy transfer. Assuming that the activated

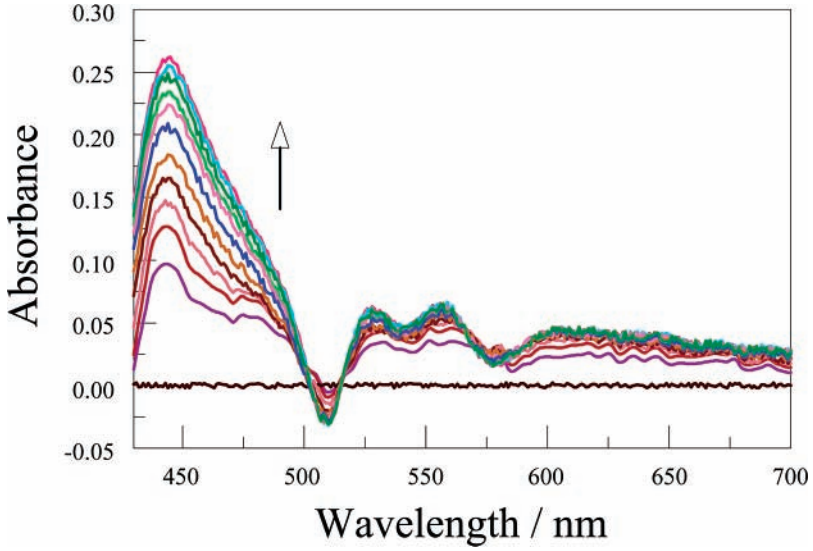

Figure 7. Transient absorption spectra recorded after laser excitation of dyad **D1** at 590 nm. Note that the signal at ~440 nm increases as the delay time increases.

process refers to electron exchange, it is more appropriate to express k_1 ($k_1 = k_{TT} - k_0$) in the following Arrhenius-type expression (Figure 6b).[26]

$$k_1\sqrt{T} = \frac{2\pi}{\hbar}|V_{DA}|^2\frac{1}{\sqrt{4\pi k_B\lambda}}\exp\left(-\frac{\Delta G^{\#}}{k_B T}\right) \qquad (2)$$

Here, V_{DA} is the electronic coupling matrix element, $\Delta G^{\#}$ is the change in free energy of activation, and λ is the reorganization energy accompanying electron exchange. The pre-exponential factor corresponds to the upper limit for electron exchange and has a value of 4×10^{12} s^{-1} at room temperature. This value seems appropriate for energy transfer across a relatively short distance.[27] The derived activation energy of 0.19 eV can be used to estimate a value for the reorganization energy on the basis that reaction occurs within the framework of Marcus theory.[28] Thus, taking the change in Gibbs free energy ($\Delta G°$) as being equal to the difference in triplet energies between the MLCT state and the porphyrin T_1 state ($\Delta G° = -0.46$ eV), the reorganization energy becomes 1.54 or 0.14 eV. Given that the reorganization energy associated with intramolecular triplet energy transfer is usually small,[29] we prefer to accept the latter value. On this basis, triplet energy transfer occurs within the Marcus inverted region.[28] Furthermore, the pre-exponential factor can now be used to estimate the magnitude of the electronic coupling matrix element (V_{DA}) for electron exchange. The derived value ($V_{DA} = 0.0094$ eV or 76 cm^{-1}) is relatively high[30] and suggests that the reactants remain in modest electronic coupling, despite the presence of the bridging terpyridine unit. The activationless process (k_0), which also relates to triplet−triplet energy transfer, can be assigned to nuclear tunneling.[31] This effect is favored at low temperature and for reactions occurring within the inverted Marcus regime.

$$\Delta G^{\#} = \frac{(\Delta G° + \lambda)^2}{4\lambda} \qquad (3)$$

Selective Excitation into the Q-band of the Porphyrin Moiety. Illumination of dyad **D1** at 570 nm, where the Q-band localized on the free-base porphyrin is the dominant chromophore (see Figure 2), results in emission from the first-excited singlet (S_1) state of the porphyrin subunit. The emission spectra recorded for **D1** (Figure 4) remains very similar to that of the reference compound **R1**. However, fluorescence recorded for **D1** is strongly quenched, with respect to the reference. Indeed, the relative quantum yields indicate that fluorescence from the S_1 level of the porphyrin is only 2.7% that of the reference compound. The emission lifetime ($\tau_s = 260$ ps) is similarly reduced, relative to that recorded for **R1** ($\tau_s = 7.3$ ns); both fluorescence decay profiles were monoexponential at room temperature. Comparing the photophysical properties recorded for dyad **D1**, with illumination at 570 nm, with those measured for **R1** gives a quenching rate constant of $k = 1/\tau_s$(**D1**) − $1/\tau_s$(**R1**) $= 3.7 \times 10^9$ s^{-1}. This value represents efficient quenching of the S_1 state by the appended metal complex. Such behavior has been noted previously for related dyads lacking the phenylethynylene group. Thus, for the directly linked dyad,[5b,5c] the porphyrin S_1 state is quenched with a rate constant of 2.4×10^9 s^{-1} at room temperature. Quenching was attributed to singlet−triplet energy transfer from S_1 to the MLCT triplet state localized on the metal complex, although this was difficult to establish, because of the fast decay of the latter triplet. Inserting a single phenylene ring between the reactants[5a] gave a very fast rate of singlet−triplet energy transfer ($k_{ST} = 9 \times 10^9$ s^{-1}) at 77 K. At room temperature, singlet−triplet energy transfer competed with intramolecular electron transfer from S_1 to the appended metal complex. Under these conditions, $k_{ST} = 9.1 \times 10^9$ s^{-1}. The fact that energy transfer appears to be activationless in this latter dyad should not be taken as evidence that the predominant mechanism involves Förster-type interactions. Indeed, the activation energy for Dexter-type electron exchange should be very small for this system, because $\Delta G° \approx -\lambda$, whereas the close proximity of the reactants might favor fast nuclear tunneling.

For dyad **D1**, light-induced electron transfer from the porphyrin S_1 state to the metal complex is thermodynamically unfavorable ($\Delta G° = +0.11$ eV)[25] and seems unlikely to account for the efficient fluorescence quenching. Laser flash photolysis studies made at room temperature with 590 nm excitation showed that the singlet-excited state of the porphyrin was present immediately after the pulse (Figure 7). This species decayed rapidly, with a lifetime (τ_S) of 250 ps. On longer time scales, the flash photolysis records indicate the presence of the porphyrin-based π,π^* excited triplet state, as recognized by its characteristic differential absorption spectrum (see Figure 7). This triplet state decays with a lifetime of 200 μs in deoxy-

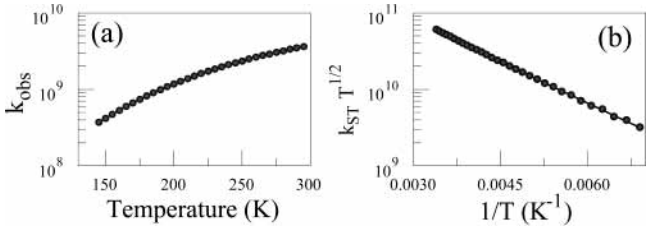

Figure 8. Effect of temperature on the rate of singlet−triplet energy transfer, following excitation of dyad **D1** at 590 nm.

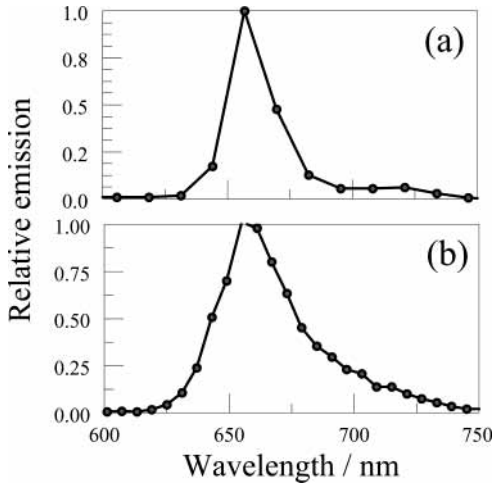

Figure 9. Time-gated emission spectra recorded at 200 K for dyad **D1** after laser excitation at 590 nm: (a) spectrum of the short-lived component and (b) spectrum of the long-lived component.

genated DMF at room temperature. At intermediate times, the transient absorption records show the presence of an additional species that is formed from S_1 and decays to give T_1. The differential absorption spectrum of this species shows pronounced bleaching at 490 nm and can be assigned to the triplet MLCT state.[15] It is formed with a rate constant of 4×10^9 s^{-1} and decays with a rate constant of 2×10^9 s^{-1}. Consequently, its steady-state concentration is minimal and, taken together with the very low emission quantum yield, explains the failure to observe this species in the luminescence experiments. It is clear that the triplet MLCT state is formed from the porphyrin S_1 state by singlet−triplet energy transfer.

The luminescence spectral profile recorded following excitation into the S_1 absorption band of the porphyrin shows a modest dependence on temperature (see Supporting Information). The total emission yield increases as the temperature decreases, but there is also a progressive change in the spectral pattern. At high temperature, the spectrum is characteristic of fluorescence from the S_1 state of the free-base porphyrin. At lower temperatures, however, the emission spectrum becomes contaminated with phosphorescence from the triplet MLCT state. The latter species does not dominate the spectral profile, at any temperature, but makes a clear contribution to the total spectrum. Indeed, the time-resolved fluorescence decay records become dual exponential as the temperature decreases. Thus, at 200 K, the best fit to the deconvoluted decay profile involves lifetimes of 880 ps (95%) and 19.2 ns (5%) (Figure 8). Time-gated spectra indicate that the shorter-lived species is the porphyrin S_1 state, whereas the longer-lived species is the triplet MLCT state localized on the metal complex (Figure 9). Both lifetimes increase as the temperature decreases. The temperature dependence for the triplet MLCT state is as described previously, whereas the rate of decay of the porphyrin S_1 state, as ascribed solely to singlet−triplet energy transfer, follows the form of eq 1 (Figure 10).

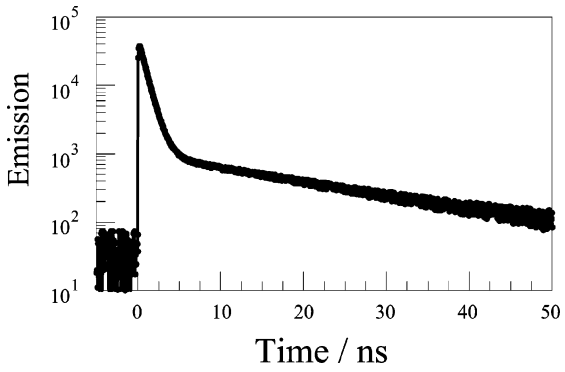

Figure 10. Time-resolved fluorescence decay profile recorded at 650 nm following laser excitation of dyad **D1** at 200 K with a laser pulse (full width at half maximum (fwhm) = 6 ps) at 590 nm.

Thus, at low temperature, the rate of singlet−triplet energy transfer approaches a temperature-independent value (k_{ST}^0) of ca. 2×10^7 s^{-1}. This value can be compared with the activationless rate constant for triplet−triplet energy transfer ($k_0 = 1.4 \times 10^7$ s^{-1}) found for the triplet MLCT state. However, note that the inherent rate constant for decay of the S_1 state of **R1** is 8.2×10^7 s^{-1} at low temperature, such that the determination of (k_{ST}^0) as the difference between two similar lifetimes is somewhat hazardous. However, support for this temperature-independent pathway is derived from the observation that the low-temperature emission spectra are contaminated with luminescence from the MLCT triplet, even for excitation at 610 nm, where the metal complex is essentially transparent. At higher temperatures, the rate of energy transfer becomes weakly activated and can be expressed in terms of eq 2. The activation energy for this latter process is 0.060 eV, which is considerably smaller than that found for the corresponding triplet−triplet energy-transfer step. The reorganization energy, calculated from eq 3 with $\Delta G° = +0.05$ eV, is $\lambda = 0.12$ eV, which is slightly lower than found for the corresponding triplet−triplet transfer. The upper limit for the rate of singlet−triplet energy transfer (k_{ACT}) at room temperature is only 9.4×10^{10} s^{-1}, which is markedly reduced, relative to the triplet process. Similarly, the coupling element is decreased to $V_{DA} = 11$ cm^{-1} (i.e., 0.00138 eV). This decrease in both V_{DA} and k_{ACT} for singlet−triplet energy transfer presumably arises because this process is spin-forbidden, despite the presence of the heavy atom. Given that electronic coupling is relatively weak for singlet−triplet energy transfer, it seems unlikely that the temperature-independent step can be attributed to nuclear tunneling. Instead, it is possible that this behavior reflects the onset of Förster-type energy transfer at low temperature. The derived rate constant is significantly lower than that for electron exchange at room temperature, such that the latter mechanism is dominant.

Excitation into the Soret Band of the Porphyrin Subunit. Excitation of the reference porphyrin **R1** at 380 nm, which corresponds to the upper vibrational level of the second-excited singlet (S_2) state, results in the appearance of very weak fluorescence from the Soret band. The relative fluorescence yield recorded in the Soret region (400−520 nm) for dyad **1**, with respect to **R1**, is approximately unity, which is in marked contrast to the situation described previously for S_1 fluorescence. The close comparability found for emission yields from the S_2 levels of the **D1** dyad and the reference compound **R1** indicates that internal conversion is too fast in the free-base porphyrin to

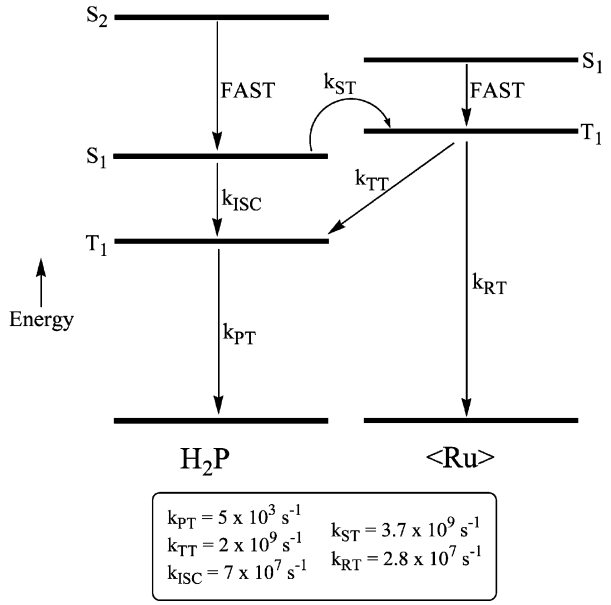

Figure 11. Energy level diagram showing the various energy-transfer steps occurring in dyad **D1**.

allow competitive electron-transfer or energy-transfer processes. This situation is confirmed by the fact that the corrected excitation and absorption spectra agree very well in the Soret region.

Concluding Remarks

The appended metal complex harvests photons in the 440−530 nm region, where the free-base porphyrin is relatively transparent, and acts as an energy relay to promote intersystem crossing in the porphyrin (Figure 11). There is no evidence for either light-induced electron transfer or through-space energy transfer in dyad **D1**. Instead, energy transfer occurs via Dexter-type electron exchange and is weakly activated. Such processes occur in a frozen glass, at rates comparable to those found in fluid solution, and the efficiency is ∼100% in all cases. The triplet MLCT state associated with the proximal terpyridine ligand is a possible "virtual" intermediate in both energy-transfer steps, because electron exchange must cross this unit. The average torsion angle between the porphyrin nucleus and the bridging phenylene ring is 44°, and this might impose a barrier to through-bond electron exchange. Singlet−triplet and triplet−triplet energy-transfer steps differ markedly in terms of the size of the electronic coupling matrix elements and the upper limits for electron exchange at room temperature. This disparity reflects the fact that singlet−triplet energy transfer is spin-forbidden. Interestingly, note that, in both cases, the transfer mechanism changes at low temperature. Nuclear tunneling occurs in the triplet−triplet energy-transfer step as the medium freezes. Such behavior is not unusual for reactions that occur in the Marcus inverted region at low temperature.[31] For singlet−singlet energy transfer, there is a gradual shift from electron exchange to the dipole−dipole mechanism as the temperature decreases. This situation ensures that energy transfer is efficient in a frozen glass at 77 K.

Acknowledgment. We thank the EPSRC (GR/R92615/01) and the University of Newcastle for their financial support of this work.

Supporting Information Available: Temperature-dependent emission spectra are provided for various excitation wavelengths, together with plots of emission quantum yield versus temperature. Also shown is a time profile for each transient species formed after selective excitation into the Q-band of the porphyrin. A table of measured lifetimes for dyad **D1** and **R2** at different temperatures is provided. (PDF.) This material is available free of charge via the Internet at http://pubs.acs.org.

References and Notes

(1) (a) Harriman, A.; Sauvage, J.-P. *Chem. Soc. Rev.* **1996**, *34*, 849. (b) Collin, J.-P.; Harriman, A.; Heitz, V.; Odobel, F.; Sauvage, J.-P. *Coord. Chem. Rev.* **1996**, *148*, 63.

(2) (a) Hamilton, A. D.; Rubin, H.-D.; Bocarsly, A. B. *J. Am. Chem. Soc*. **1984**, *106*, 7255. (b) Sessler, J. L.; Capuano, V. L.; Burrell, A. K. *Inorg. Chim. Acta* **1993**, *204*, 93. (c) Araki, K.; Torma, H. E. *J. Photochem. Photobiol. A: Chem.* **1994**, *83*, 245. (d) Collin, J.-P.; Dalbavie, J.-O.; Heitz, V.; Sauvage, J.-P.; Flamigni, L.; Armaroli, N.; Balzani, V.; Barigelletti, F.; Montanari, I. *Bull. Soc. Chim. Fr.* **1996**, *133*, 749. (e) Kimura, M.; Hamakawa, T.; Muto, T.; Hanabusa, K.; Shirai, H.; Kobayashi, N. *Tetrahedron Lett.* **1998**, *39*, 8471. (f) Dixon, I. M.; Collin, J.-P. *J. Porphyrins Phthalocyanines* **2001**, *5*, 600. (g) Bruce, J. I.; Chambron, J.-C.; Kolle, P.; Sauvage, J.-P. *J. Chem. Soc., Perkin Trans. 1* **2002**, 1226.

(3) Chichak, K.; Branda, N. R. *Chem. Commun*. **1999**, 523.

(4) Norsten, T. B.; Chichak, K.; Branda, N. R. *Tetrahedron* **2002**, *58*, 639.

(5) (a) Flamigni, L.; Armaroli, N.; Barigelletti, F.; Balzani, V.; Collin, J.-P.; Dalbavie, J.-O.; Heitz, V.; Sauvage, J.-P. *J. Phys. Chem. B* **1997**, *101*, 5936. (b) Flamigni, L.; Barigelletti, F.; Armaroli, N.; Collin, J.-P.; Sauvage, J.-P.; Williams, J. A. G. *Chem. Eur. J*. **1998**, *4*, 1744. (c) Flamigni, L.; Barigelletti, F.; Armaroli, N.; Ventura, B.; Collin, J.-P.; Sauvage, J.-P.; Williams, J. A. G. *Inorg. Chem*. **1999**, *38*, 661.

(6) Harriman, A.; Hissler, M.; Trompette, O.; Ziessel, R. *J. Am. Chem. Soc*. **1999**, *121*, 2516.

(7) (a) Odobel, F.; Sauvage, J.-P. *New J. Chem*. **1994**, *18*, 1139. (b) Harriman, A.; Odobel, F.; Sauvage, J.-P. *J. Am. Chem. Soc*. **1995**, *116*, 5481. (c) Harriman, A.; Odobel, F.; Sauvage, J.-P. *J. Am. Chem. Soc*. **1995**, *117*, 9461.

(8) Flamigni, L.; Marconi, G.; Dixon, I. M.; Collin, J.-P.; Sauvage, J.-P. *J. Phys. Chem. B* **2002**, *106*, 6663.

(9) Uyeda, H. T.; Zhao, Y.; Wostyn, K.; Asselberghs, I.; Clays, K.; Persoons, A.; Therien, M. J. *J. Am. Chem. Soc*. **2002**, *124*, 13806.

(10) (a) Collin, J. P.; Heitz, V.; Sauvage, J.-P. *Tetrahedron Lett*. **1991**, *32*, 5977. (b) Collin, J.-P.; Harriman, A.; Heitz, V.; Odobel, F.; Sauvage, J.-P. *J. Am. Chem. Soc*. **1994**, *116*, 5679. (c) Crossley, M. J.; Burn, P. L.; Langford, S. J.; Prashar, J. K. *J. Chem. Soc., Chem. Commun*. **1995**, 1921. (d) Vannelli, T. A.; Karpishin, T. B. *Inorg. Chem*. **1999**, *38*, 2246. (e) Vannelli, T. A.; Karpishin, T. B. *Inorg. Chem*. **2000**, *39*, 340.

(11) Winkler, J. R.; Netzel, T. L.; Creutz, C.; Sutin, N. *J. Am. Chem. Soc*. **1987**, *109*, 2181.

(12) (a) Benniston, A. C.; Grosshenny, V.; Harriman, A.; Ziessel, R. *Angew. Chem., Int. Ed. Engl*. **1994**, *33*, 1884. (b) Grosshenny, V.; Harriman, A.; Romero, F. M.; Ziessel, R. *J. Phys. Chem*. **1996**, *100*, 17472.

(13) (a) Newman, M. S.; Lee, L. F. *J. Org. Chem*. **1972**, *37* (26), 4468. (b) Beavington, R.; Burn, P. L. *J. Chem. Soc., Perkin Trans. 2* **1999**, 583.

(14) (a) Collin, J.-P.; Guillerez, G.; Sauvage, J.-P., Barigelletti, F.; De Cola, L.; Flamigni, L.; Balzani, V. *Inorg. Chem*. **1991**, *30*, 4230. (b) Spahni, W.; Calzaferri, G. *Helv. Chim. Acta* **1984**, *67*, 450.

(15) Benniston, A. C.; Chapman, G.; Harriman, A.; Mehrabi, M.; Sams, C. A. *Inorg. Chem*. **2004**, *43* (14), 4227.

(16) Sven, H. F.; Wilson, S. W.; Pomerantz, M.; Walsh, J. L. *Inorg. Chem*. **1989**, *28*, 786.

(17) Harriman, A.; Hosie, R. J. *J. Chem. Soc., Faraday Trans. 2* **1981**, *77*, 1695.

(18) (a) Demas, J. N.; Crosby, G. A. *J. Am. Chem. Soc*. **1971**, *93*, 2841. (b) Kober, E. M.; Marshall, J. L.; Dressick, W. J.; Sullivan, B. P.; Caspar, J.-V.; Meyer, T. J. *Inorg. Chem*. **1985**, *24*, 2755.

(19) (a) Lindsey, J. S.; Hsu, H. C.; Schreiman, I. C. *Tetrahedron Lett*. **1986**, *27*, 4969. (b) Lindsey, J. S.; Schreiman, I. C.; Hsu, H. C.; Kearney, P. C.; Marguerettaz, A. M. *J. Org. Chem*. **1987**, *52*, 827. (c) Lindsey, J. S.; Wagner, R. W. *J. Org. Chem*. **1989**, *54*, 828.

(20) The energy-minimized structure was obtained by molecular mechanics methods using MOPAC.

(21) (a) Hissler, M.; El-Ghayoury, A.; Harriman, A.; Ziessel, R. *Angew. Chem., Int. Ed. Engl*. **1998**, *37*, 1717. (b) Hissler, M.; El-Ghayoury, A.; Harriman, A.; Ziessel, R. *Coord. Chem. Rev*. **1998**, *178*, 1251.

(22) Benniston, A. C.; Harriman, A.; Ziessel, R. *J. Chem. Soc., Dalton Trans*. **2004**, 1227.

(23) Amini, A.; Harriman, A.; Mayeux, A. *Phys. Chem. Chem. Phys*. **2004**, *6*, 1157.

(24) Harriman, A. *J. Chem. Soc., Faraday Trans. 2* **1981**, *77*, 1288.

(25) Calculated according to the relation $\Delta G^\circ = \Delta G_\pm - E_S$, where E_S is the excitation energy of the excited state and $\Delta G_\pm$ is given by the following expression: $\Delta G_\pm = e(E_{OX} - E_{RED}) - e^2/(4\pi\epsilon_0\epsilon_S r_{DA})$. Here, E_{OX} and E_{RED} respectively refer to the reduction potential for one-electron oxidation of the porphyrin and one-electron reduction of the Ru-terpy subunits, r_{DA} is the separation distance between the redox-active units, and ϵ_S is the static dielectric constant of the solvent.

(26) Liu, J. Y.; Bolton, J. R. *J. Phys. Chem*. **1992**, *96*, 1718.

(27) (a) Closs, G. L.; Piotrowiak, P.; MacInnis, J. M.; Fleming, G. R. *J. Am. Chem. Soc*. **1988**, *110*, 2652. (b) Oevering, H.; Verhoeven, J.; Paddon-Row, M. N.; Cotsaris, E.; Hush, N. S. *Chem. Phys. Lett*. **1988**, *143*, 488. (c) Barigelletti, F.; Flamigni, L. *Chem. Soc. Rev*. **2000**, *29*, 1. (d) Harriman, A.; Khatyr, A.; Ziessel, R.; Benniston, A. C. *Angew. Chem., Int. Ed*. **2000**, *39*, 4287.

(28) (a) Marcus, R. A. *J. Chem. Phys*. **1956**, *24*, 966. (b) Marcus, R. A. *Faraday Discuss. Chem. Soc*. **1960**, *29*, 21. (c) Marcus, R. A. *Annu. Rev. Phys. Chem*. **1964**, *15*, 155. (d) Marcus, R. A. *J. Chem. Phys*. **1965**, *43*, 679.

(29) The reorganization energy for deactivation of the first-excited MLCT triplet state of **R2** has been calculated from emission spectral measurements as being 680 cm^{-1}. The Stokes shift for the first-excited singlet state of the free-base porphyrin reference compound is only 350. Thus, the expected reorganization energy for energy transfer in **D1** is ca. 1030 cm^{-1} (i.e., 0.13 eV). We assume that a similar value holds for triplet−triplet energy transfer.

(30) Sutin, N. In *Electron Transfer in Inorganic, Organic and Biological Systems*; Bolton, J. R., Ed.; Advances in Chemistry Series 228; American Chemical Society: Washington, DC, 1991; pp 25−43.

(31) May, V.; Kuhn, O. *Charge and Energy Transfer Dynamics in Molecular Systems*; Wiley−VCH: Berlin, 2001; Chapter 6.